Thermal Stability of W-Contacted Junction Diodes

Wen-Kuan Yeh, Kuang-Yang Chan, Ting-Chang Chang, and Mao-Chieh Chen*

Department of Electronics Engineering, National Chiao Tung University and National Nano Device Laboratory, Hsinchu, Taiwan

Mou-Shiung Lin

Taiwan Semiconductor Manufacturing Company, Hsinchu, Taiwan

ABSTRACT

This work investigates the thermal stability of W-contacted p^+n junction diodes, in which the tungsten contact was formed by selective chemical vapor deposition (CVD) or sputtering process. Reaction of Al and CVD-W at elevated temperature leads to the formation of WAl_{12}, and the barrier capability of CVD-W film was dependent on the consumption of W. The sputter-W film has a columnar structure and contains a higher content of oxygen. The presence of oxygen retarded the formation of WAl_{12} and thus enhanced the thermal stability of the Al/W/Si structure. However, degradation of the Al/sputter-W (100 nm)/p^+n diodes occurred after 30 min annealing at 550°C, presumably due to Al diffusion along the grain boundary of sputter-W film. For the CVD-W contacted junction diodes, insertion of a thin TiN barrier layer between the Al and W film was effective in suppressing the formation of WAl_{12} and thus improved the device's thermal stability.

Introduction

In very large scale integrated (VLSI) process technology, fabrication of highly reliable low contact resistance shallow junctions is of great concern. Thus, the introduction of barrier layers between the aluminum metallization and the silicon substrate is becoming increasingly important in order to avoid junction spiking and contact degradation caused by the transport of substrate silicon into the aluminum overlayer.[1] Tungsten is considered to be a good contact barrier to protect shallow junctions from aluminum spiking[2,3] and preserve low contact resistance.[4,5] However, formation of W-Al alloy, such as WAl_{12},[6,7] WAl_5 [8] or WAl_4,[9] was reported for the 450°C annealed Al/W/Si structure, and interdiffusion between Al and Si substrate after 500°C annealing was reported.[10] Nonetheless, little study has been made on the Al/W/p^+n junction diode with regard to electrical characteristics of the thermal aspects. This work investigates the thermal stability of W contacted p^+n junction diodes in which the W contact was formed by selective CVD as well as sputtering process. Furthermore, the effect of an additional thin TiN layer as a diffusion barrier was also investigated.

Experimental

The starting material was n-type <100> oriented Si wafers with 10 to 20 Ω-cm nominal resistivity. After RCA standard cleaning, the wafers were thermally oxidized to grow a 4000 Å oxide layer. Diffusion areas with a size of 100 × 100 μm were defined on the oxide-covered wafers using the conventional photolithographic technique. The p^+n junctions were formed by BF_2^+ implantation at 30 keV to a dose of 3 × 10^{15} cm^{-2} followed by furnace annealing at 900°C for 30 min in N_2 ambient. A 4000 Å of tetraethylorthosilicate (TEOS) layer was then deposited on the wafers, and contact holes with sizes ranging from 1.2 to 3 μm were defined using the conventional photolithographic technique, such that each diffusion region (with an area of 100 × 100 μm) contains a total of 25 contacts. The wafers were split into four groups for the preparation of the following W contacted junction diodes: sputter-W/p^+n, CVD-W (100 nm)/p^+n, CVD-W (300 nm)/p^+n, and TiN/CVD-W (300 nm)/p^+n. The sputter-W film was deposited using dc magnetron sputtering in Ar ambient at a pressure of 8 mTorr and with a deposition a rate of 3 nm/min. The CVD-W films were deposited using the selective CVD-W technique with the process of silane reduction of WF_6 conducted with conditions illustrated as follows: substrate temperature

300°C, total gas pressure 0.1 Torr, WF_6 flow rate 20 sccm, SiH_4 flow rate 10 sccm, and H_2 carrier gas flow rate 1000 sccm. The CVD-W films of two different thicknesses, 100 and 300 nm, were deposited. Part of the samples with 300 nm CVD-W films were further deposited with a 40 nm of TiN layer; the TiN deposition was carried out by reactive sputtering a pure Ti target in mixed Ar/N_2 (7/1) ambient at a pressure of 5 mTorr. Finally, Al metallization was applied to all samples, followed by 30 min sintering at 400°C. For the thermal stability study of the diodes, the samples were thermally annealed in N_2 flowing furnace for 30 min at a temperature ranging from 400 to 600°C. Contact resistance of the junction diodes was measured using the four-terminal Kelvin structure. X-ray diffraction (XRD) analysis was used for crystalline-phase identification. Scanning electron microscopy (SEM) was employed to inspect the change of microstrcture, and secondary ion mass spectroscopy (SIMS) was used to measure the depth profile of atomical composition. The x-ray photoelectron spectroscopy (XPS) was used to analyze the Al/W interface.

Results and Discussion

Figure 1 shows the statistical distributions of reverse bias leakage currents for four different structures of W contacted p^+n junction diodes annealed at various temperatures. The junction characteristics of the Al/CVD-W (300 nm)/p^+n junction diodes were stable up to 550°C (Fig. 1c$_3$), while those of the Al/CVD-W (100 nm)/p^+n and Al/sputtered-W (100 nm)/p^+n junction diodes were severely degraded (Fig. 1a$_4$ and 1b$_3$). It is clear that the thermal stability of the Al/CVD-W/p^+n diodes was substantially improved by using a thicker W film. In addition, insertion of a TiN layer between Al and W further improved the diode's thermal stability and a majority of the Al/TiN/CVD-W (300 nm)/p^+n diodes (>50%) remained stable up to 600°C (Fig. 1d$_4$). The degradation of the Al/CVD-W/p^+n junction diodes was due to the interdiffusion between Al and Si (which was confirmed later in Fig. 8), but the formation of WAl_{12} retarded the diffusion of Al until the W layer was entirely consumed. The x-ray diffraction patterns for the Al/CVD-W/Si samples are illustrated in Fig. 2 and 3. For the Al/CVD-W (100 nm)/Si sample, the WAl_{12} signal appeared after 500°C annealing, and was accompanied by the diminution of the α-W signal. After 550°C annealing, the W signal further weakened, while various signals of WSi_2 phase appeared. For the Al/CVD-W (300 nm)/Si sample, weak signals fo the WAl_{12} phase were found after 575°C annealing. It was presumed
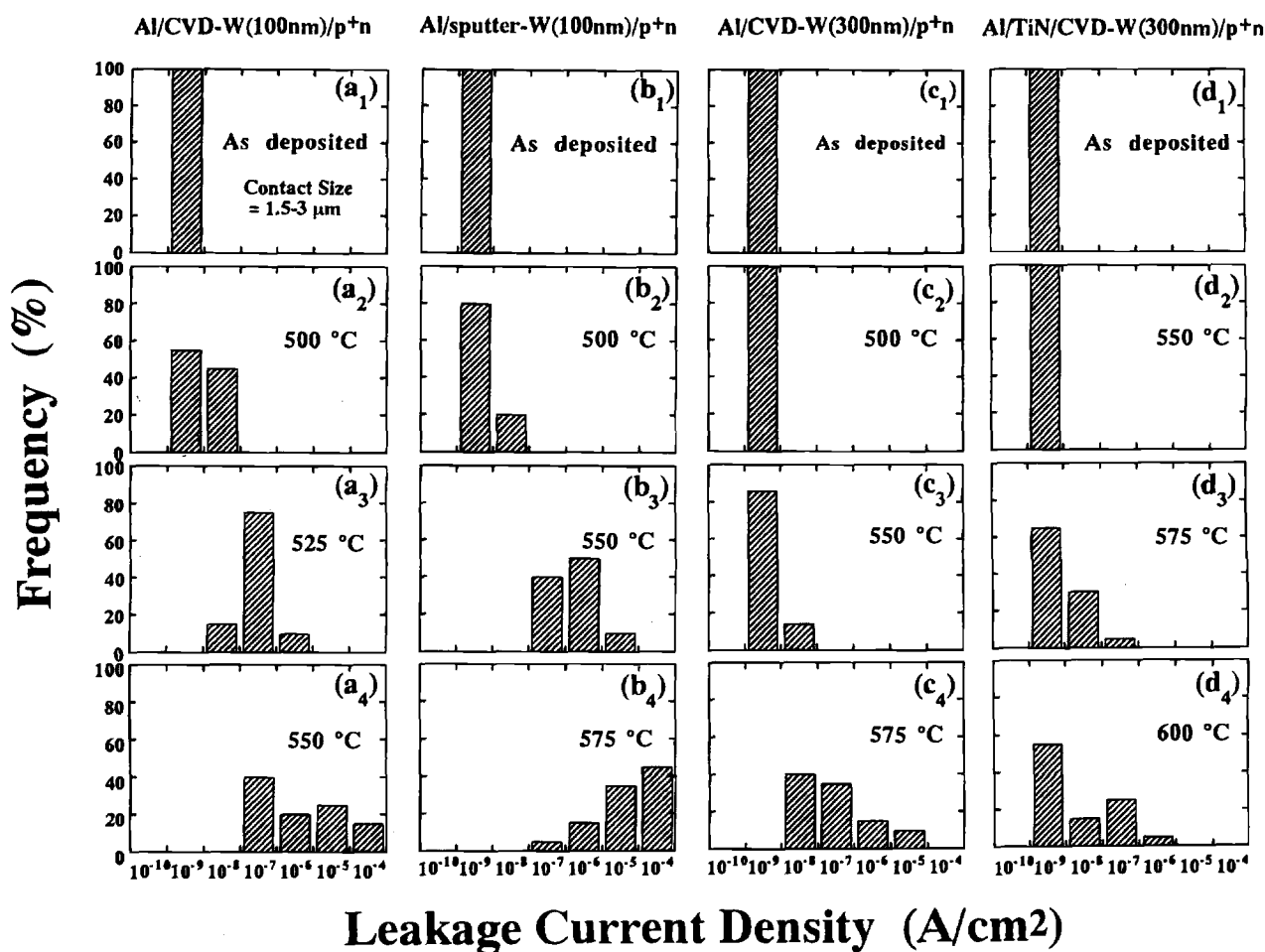
* Electrochemical Society Active Member.

Fig. 1. Histograms showing the distribution of reverse leakage current density measured at -5 V for (a) Al/CVD-W (100 nm)/p^+n, (b) Al/sputter-W (100 nm)/p^+n, (c) Al/CVD-W (300 nm)/p^+n, and (d) Al/TiN (40 nm)/CVD-W (300 nm)/p^+n junction diodes annealed at various temperatures.

that the thin W film of 100 nm was almost entirely consumed by the formation of WAl_{12} after the 550°C anneal leading to severe junction degradation of the Al/CVD-W (100 nm)/p^+n diodes due to Al diffusion into the Si substrate. For the W film of 300 nm thickness, part of the W layer was converted into WAl_{12} after the 550°C anneal for 30 min; thus, electrical characteristics of the Al/CVD-W (300 nm)/p^+n diodes basically remained stable up to 550°C. Figure 4 shows the x-ray diffraction patterns of the Al/sputter-W (100 nm)/Si sample, in which the β-W and the broadened α-W peaks were observed. In contrast with the sample composed of sputter-W; instead it appeared after 575°C annealing. Apparently, the formation of WAl_{12} was retarded for the sputter-W film. Figure 5 shows the cross section and top view SEM micrographs for the four different W contacted multilayer structures after 550°C annealing. It is shown that most of the 100 nm CVD-W film was consumed to form the WAl_{12} compound and thus its barrier capability was lost against Al diffusion (Fig. 5a$_1$ and 5a$_2$). The columnar structure of the sputter-W film (Fig. 5b$_2$) belongs to β-type W structure,[11] which contains a large number of grain boundaries; the grain boundary acts as a diffusion path of Al into the Si substrate. Many pinholes can be seen on the surface of the Al/sputter-W/Si sample (Fig. 5b$_1$), though the sputter-W/Si interface looked nearly unchanged. Thus, for the Al/sputter-W/p^+n diodes, it is presumed that the degradation of junction was due to Al diffusion along the grain boundary of sputter-W film into the Si substrate. The Al/CVD-W (300 nm)/Si

samples did not degrade after 550°C anneal because the thicker W film was only partially consumed and the W/Si interface remained unchanged (Fig. 5c$_1$ and 5c$_2$). With the insertion of a TiN layer between Al and W, it was possible to suppress the WAl_{12} compound formation, keeping the W/Si interface as well as the Al surface unchanged up to 550°C (Fig. 5d$_1$ and 5d$_2$).

Figure 6 shows the increase of sheet resistance for the various W contacted structures as a function of annealing temperature. Below 450°C, all samples remained stable. At 500°C, sheet resistance of the Al/CVD-W (100 nm)/Si sample revealed a drastic increase, while that of the other samples still remained fairly stable. Slight degradation was observed for the Al/sputter-W (100 nm)/Si sample at 550°C, while sheet resistance of the Al/TiN/CVD-W (300 nm)/Si sample basically remained stable. The increase of sheet resistance may reflect the consumption of conductive aluminum due to the formation of WAl_{12}. For the Al/CVD-W (100 nm)/Si sample, the WAl_{12} compound was formed after the 500°C anneal leading to the increase of sheet resistance. After the 550°C anneal, the thin CVD-W was largely consumed resulting in mass transport of Al in Si, which can be understood from Fig. 8 shown later in this section; thus, sheet resistance of the sample further increased drastically. For the Al/CVD-W (300 nm)/Si sample, the increase of sheet resistance was due only to the formation of WAl_{12}. For the Al/sputter-W/Si sample, higher oxygen content in the sputter-W film (which was confirmed and is shown in Fig. 7) retarded the formation of
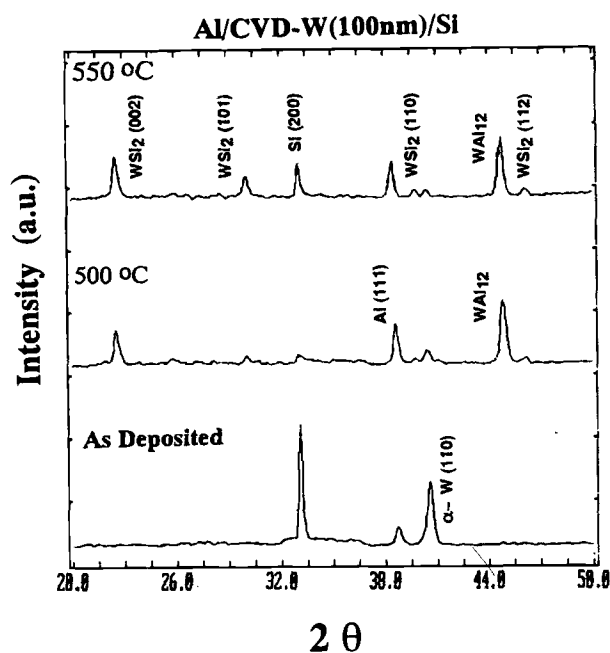
Al/CVD-W(100nm)/Si

Fig. 2. XRD spectra of Al/CVD-W (100 nm)/Si sample before and after thermal annealing.
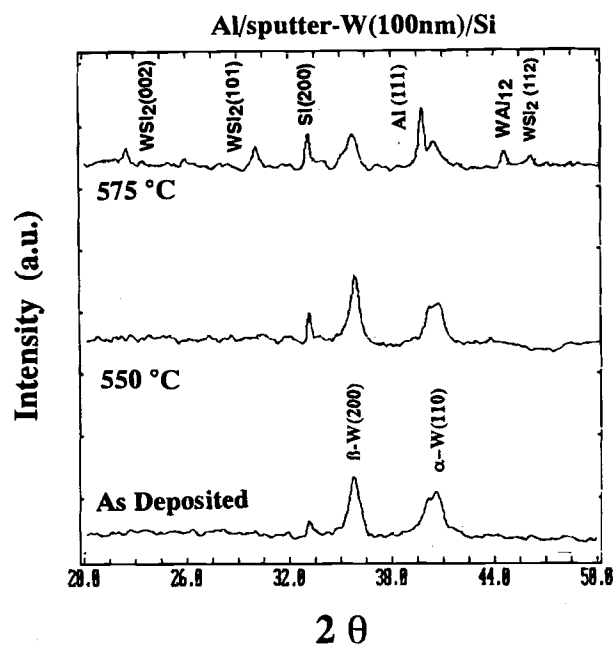
Al/sputter-W(100nm)/Si

Fig. 4. XRD spectra of Al/sputter-W (100 nm)/Si sample before and after thermal annealing.

WAl_{12}; the slight increase of sheet resistance after the 550°C anneal was presumably due to the formation of WAl_{12} as well as aluminum oxide. Figure 7 shows the results of XPS analysis for the 550°C annealed Al/sputter-W/Si and Al/CVD-W/Si samples with respect to the O_{1s}, W_{4f}, and Al_{2p} spectra. Each spectrum was taken after 2 min of Ar^+ ion milling to pre-etch the Al surface, which corresponds to a removal of about 20 nm Al from the surface. In this work, the total sputtering time was 10 min, when the ion reached the Al/W interface. For the Al/sputter-W/Si samples, O_s peak [binding energy (B.E.) = 532.14 eV]

increased with sputtering time of ion milling (Fig. 7a₁); in contrast, the O_{1s} peak for the Al/CVD-W/Si samples (B.E. = 532.6 eV) decayed with sputtering time (Fig. 7b₁). Apparently, there is an oxygen accumulation at the Al/sputter-W interface, but not at the Al/CVD-W interface. The presence of oxygen in the sputter-W film will retard the formation of WAl_{12} leading to improved thermal stability of the Al/sputter-W interface. For the W signal, the XPS analysis showed that both the $W4f_{7/2}$ peak (B.E. = 30.981 eV for CVD-W and B.E. = 31.092 eV for sputter-W) and $W4f_{5/2}$ peak (B.E. = 33.216 eV for both samples) increased with sputtering time until the W surface was reached (Fig. 7a₂ and Fig. 7b₂). For the Al signal, a doublet Al_{2p} signal was observed for the Al/sputter-W/Si sample; one of the doublets occurred at 72.75 eV [Al(1)] corresponding to the metallic Al,[12] while the second one shifted 2.9 eV toward higher energy [Al(2); B.E. = 75.65 eV] characterizing the aluminum oxide (Fig. 7a₃). Various shifts, between 2.5 and 3.5 eV for the B.E. values of the Al_{2p} peaks, have been reported for the aluminum oxide depending on the structure of the films[13] For the Al/CVD-W/Si sample, only one metallic Al_{2p} signal [Al(1); B.E. = 72.43 eV] was detected (Fig. 7b₃).

The SIMS depth profiles were used to reveal the elemental distributions in multilayered structures. Figure 8 shows the SIMS depth profiles of the four different Al/W/Si structures before and after the 550°C anneal. The interdiffuion of Al and Si led to severe degradation of the Al/CVD-W (100 nm)/Si structure after the 550°C anneal, as shown in Fig. 8a, where the W layer was transformed almost entirely into WAl_{12} and has lost its barrier capability against the Al diffusion. The barrier property of the sputter-W is much better than that of the CVD-W, as shown in Fig. 8b; this is presumbly due to high oxygen content in the sputter-W film which retarded the formation of WAl_{12}. For the Al/CVD-W (300 nm)/Si sample, interdiffusion of Al and W still occurred at the Al/W interface after 550°C annealing, but the W/Si interface remained nearly unchanged, as shown in Fig. 8c. The insertion of a TiN layer between the Al and W layers was effective in keeping the W and Si depth profiles almost unchanged, while the Al diffused only slightly into the W film, as shown in Fig. 8d. It has been reported that the composition of the reactively sputter deposited TiN is off
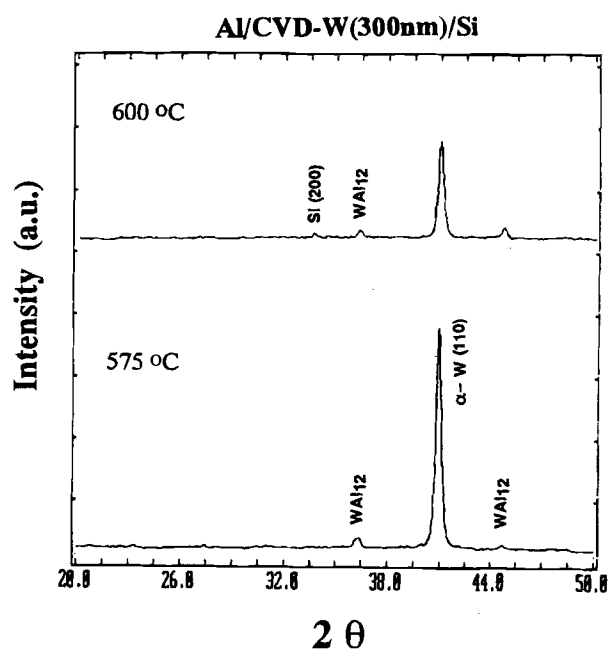
Al/CVD-W(300nm)/Si

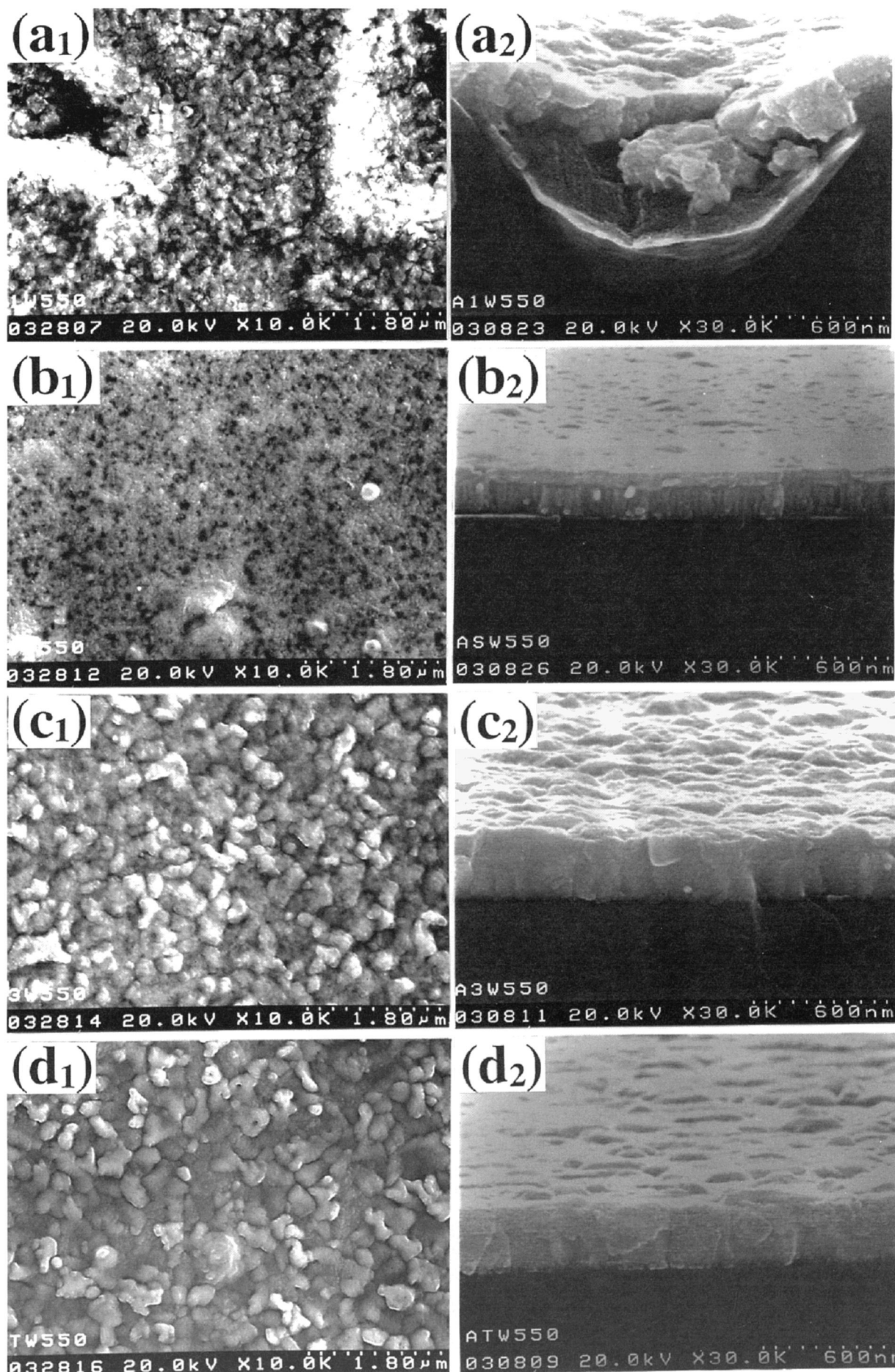Fig. 3. XRD spectra of Al/CVD-W (300 nm)/Si sample before and after thermal annealing.

Fig. 5. Top view (left) and cross section (right) SEM micrographs of (a_1, a_2) Al/CVD-W (100 nm)/Si, (b_1, b_2) Al/sputter-W (100 nm)/Si, (c_1, c_2) Al/CVD-W (300 nm,)/Si, and (d_1, d_2) Al/TiN (40 nm)/CVD-W (300 nm)/Si samples after 550°C anneal for 30 min.
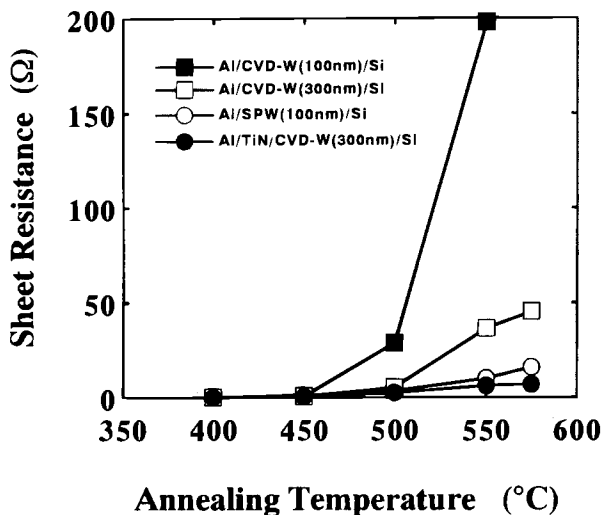
Fig. 6. Sheet resistance *vs.* annealing temperature for various diode structures.

stoichiometric,[14] thus Al could reach the W surface along the grain boundary of the TiN layer. Another possible cause of degradation in the Al/TiN/W/Si structure is due to

AlN or $TiAl_3$ [15] formation after 550°C annealing. Therefore, it is important to deposit the TiN film with the minimum amount of excess Ti[14] or with N-rich TiN.[16]

Contact resistivities of the Al/TiN/CVD-W/p^+n diodes were found to be slightly higher than those of the Al/CVD-W/p^+n diodes, which is around 5×10^{-7} Ω cm². For the Al/sputter-W/p^+n diodes, contact resistivity larger than 10^{-6} Ω cm² was obtained, presumably because native oxide on the Si substrate was not completely removed prior to the sputter-W deposition. With annealing at elevated temperatures, thermal stability of contact resistance for the Al/CVD-W/p^+n diodes depends on the thickness of W film. Figure 9 shows the increase of contact resistance as a function of annealing temperature. With a CVD-W layer of 300 nm thickness, the contact resistance could remain stable only up to 500°C. However, with the insertion of a 40 nm TiN layer, contact resistance of the Al/TiN/CVD-W (300 nm)/p^+n diode was not changed up to 575°C. The degradation behavior of the contact resistance is similar to that of the sheet resistance. The TiN layer efficiently suppressed the formation of WAl_{12} and thus improved the thermal stability of the W-contacted Al/TiN/CVD-W/p^+n diode.

Conclusion

Thermal stability of the W contacted p^+n junction diodes was investigated. Reaction of Al and CVD-W at ele-
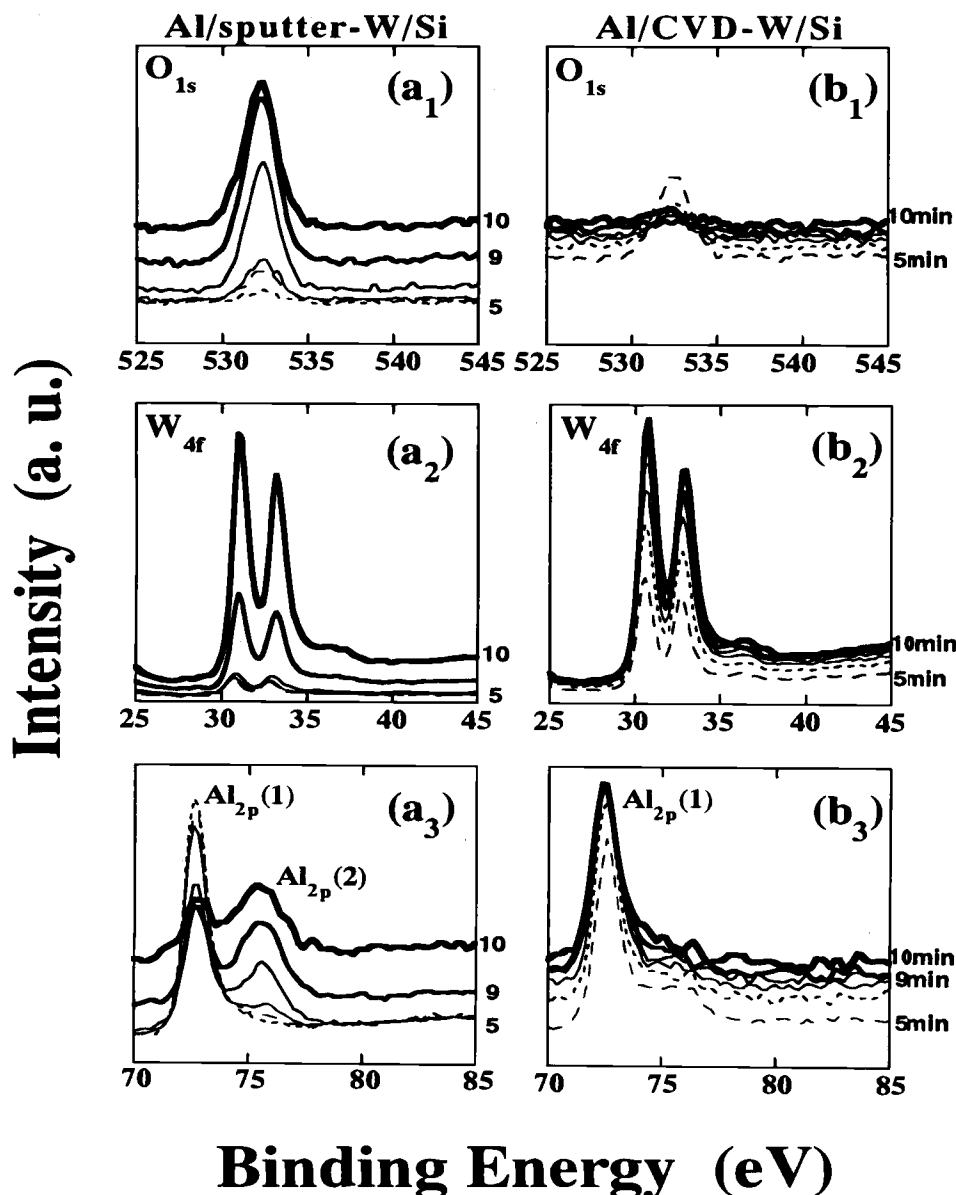

Fig. 7. XPS spectra of (a) Al/sputter-W/Si and (b) Al/CVD-W/Si multilayers after 550°C annealing. The sputtering times are indicated on the edge of each illustration.
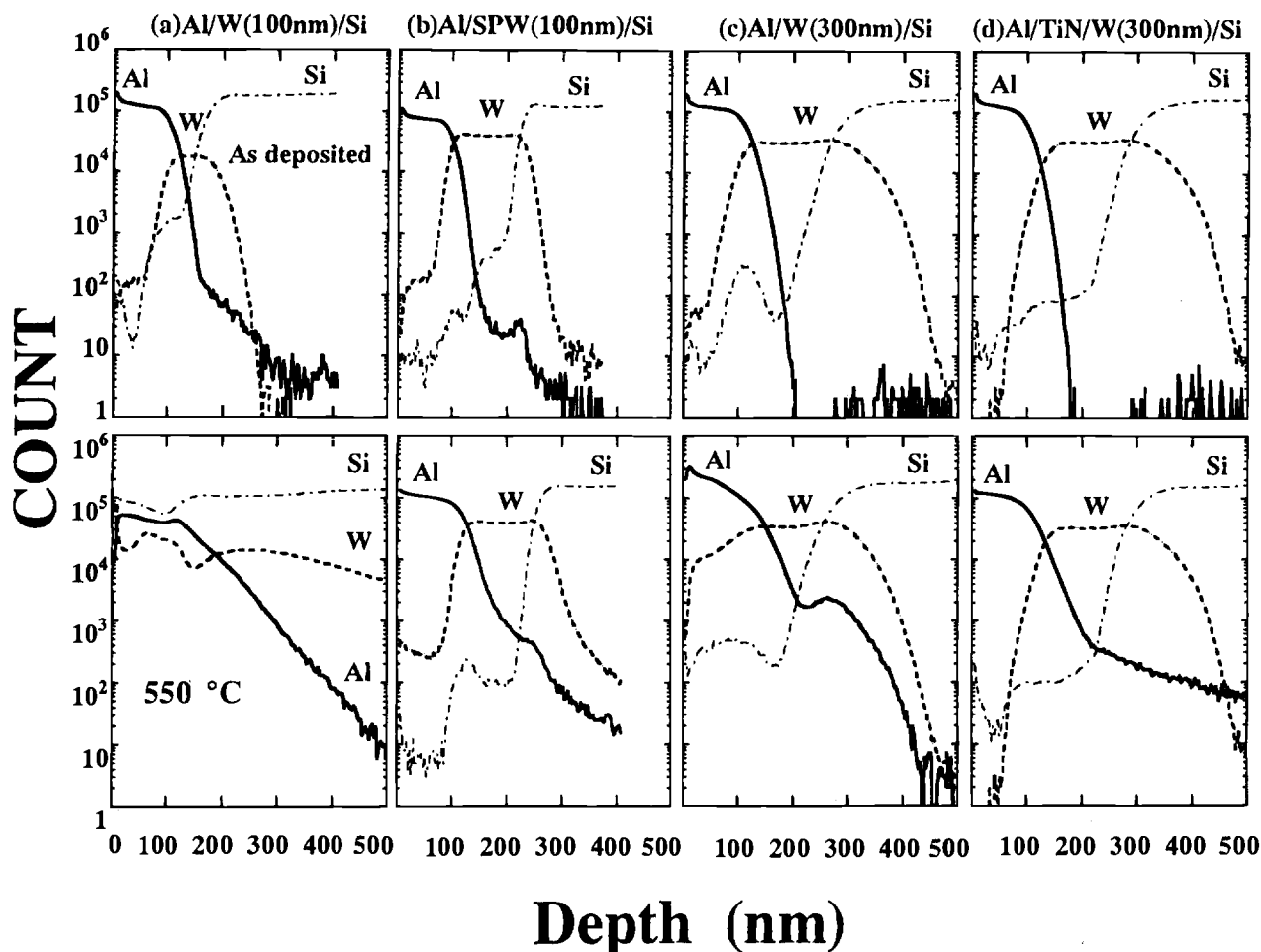
Fig. 8. SIMS depth profiles of (a) Al/CVD-W (100 nm)/Si, (b) Al/sputter-W (100 nm)/Si, (c) Al/CVD-W (300 nm)/Si, and (d) Al/TiN (40 nm)/CVD-W (300 nm)/Si samples before and after thermal annealing.

vated temperature leads to the formation of WAl_{12}, and the barrier capability of CVD-W film against Al diffusion into the Si substrate was dependent on the consumption of W. The barrier effect of sputter-W film is superior to that of CVD-W film owing to the fact that the sputter-W contains a higher content of oxygen, which retarded the formation of WAl_{12} during the high-temperature anneal. The junction

degradation occurred on the 550°C/30 min annealed Al/sputter-W (100 nm)/p^+n diodes is presumably due to Al diffusion through the grain boundary of sputter-W film, which has a columnar W structure. The insertion of a thin TiN barrier layer between the Al and CVD-W film suppressed the formation of WAl_{12} and thus improved the thermal stability of the W contacted p^+n diodes.

Fig. 9. Contact resistance vs. annealing temperature for various diode structures.

REFERENCES

1. N. E. Miller and I. Beinglass, *Solid State Technol.*, **23**, 79 (1980).
2. T. Hara, S. Enomoto, N. Ohtsuka, and S. Shima, *Jpn. J. Appl. Phys.*, **24**, 828 (1985).
3. L. Gutai, M. Delfino, and J. M. De Blasi, *Mater. Res. Soc. Symp. Proc.*, **178**, 265 (1987).
4. R. V. Levy, M. L. Green, P. K. Gallagher, and Y. S. Ali, *This Journal*, **133**, 1905 (1986).
5. Y. Shioya, M. Maeda, and K. Yanaida, *J. Vac. Sci. Technol.*, **B4**, 1175 (1986).
6. M. Hammar, S. L. Zhang, R. Buchta, and T. Johansson, *Thin Solid Films*, **185**, 9 (1990).
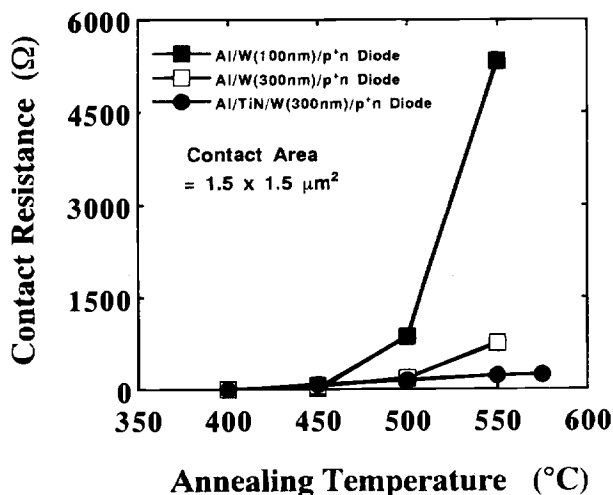7. Y. Pauleau, F. C. Dassapa, P. Lami, J. C. Oberlin, and F. Romagna, *J. Vac. Sci. Technol*, **B6**, 817 (1988).

8. H. H. Hoang, *Proc. IRPS*, p. 273 (1988).
9. P. H. Chang and H. M. Chen, *J. Appl. Phys.*, **72,** 2739 (1992).
10. B. W. Shen and G. C. Smith, *J. Vac. Sci. Technol,* **B4,** 1369 (1986).
11. Y. Harada, H. Onoda, and S. Madokoro, *Mater. Res. Soc. Symp. Proc.*, **181,** 615 (1990).
12. C. Jimenez, M. Fernandez, J. M. Albella, and J. M. Duart, *Appl. Surf. Sci.*, **70,** 475 (1993).

13. J. Avila and J. L. Sacedon, *J. Vac. Sci. Technol.*, **A10,** 2698 (1992).
14. K. Hinode and Y. Homma, *Proc. IRPS*, p. 25 (1990).
15. Y. Inoue, S. I. Tanimoto, K. Tsujimura, T. Yamashita, Y. Ibara, Y. Yamashita, and K. Yoneda, *This Journal,* **141,** 1056 (1994).
16. S. Q. Wang, I. Raaijmakers, B. J. Burrow, S. Suthar, S. Redkar, and K. B. Kim, *J. Appl. Phys.*, **68,** 5176 (1990).

Orientation Control of Chemical Vapor Deposition TiN Film for Barrier Applications

R. W. Fiordalice, R. I. Hegde, and H. Kawasaki

Motorola, Incorporated, Advanced Products Research and Development Laboratory, Austin, Texas 78721, USA

ABSTRACT

A chemical vapor deposition (CVD) TiN film with preferred <111> crystal orientation was developed using an *in situ* two-step process scheme. A thin CVD TiN layer is deposited first under low $TiCl_4$ partial pressure. This layer has poor step coverage, but acts as a crystallographic seed layer for the subsequent CVD TiN layer deposited under high $TiCl_4$ partial pressure. This layer, deposited sequentially without breaking vacuum, shows a TiN <111> preferred orientation when deposited under these conditions and provides excellent step coverage. This CVD TiN layer "stack" has shown both excellent diffusion barrier properties to CVD Cu, and improved electromigration reliability relative to conventional CVD TiN using $TiCl_4/NH_3$ chemistry.

Introduction

The limitations of sputtered barriers and contacting layers have become increasingly apparent as contact feature size continues to scale down.[1-7] In response, much effort has been put into the development of barriers and contacting layers that are deposited by chemical vapor deposition (CVD). Specifically, CVD TiN has been integrated electrically into 0.5 μm static random access memory (SRAM) devices at the contact level.[2] CVD TiN films from $TiCl_4/NH_3$ chemistry have been shown to be excellent diffusion barriers between aluminum and silicon, as well as nucleation layers for CVD tungsten.[1] However, the preferred <200> crystal orientation of CVD TiN has posed a problem. The <200> orientation of the TiN has been shown to translate to the overlying aluminum interconnect, enhancing the <200> Al feature. It has been demonstrated that an enhanced <200> orientation in aluminum interconnects portends poor electromigration performance. Therefore, the underlying <200> CVD TiN film degrades electromigration performance of the overlying aluminum interconnect by translating <200> texture.

In this paper a method to control the crystal orientation of the CVD TiN layer to produce a preferred <111> orientation is discussed. Although the <111> orientation of CVD TiN from $TiCl_4/NH_3$ chemistry has been demonstrated in the past, the resulting films showed poor step coverage.[5] Through the *in situ* layering of films deposited under two distinct process conditions, we show that it is possible to retain the conformality of the film, while at the same time producing a <111> preferred crystal orientation. Further it was found that this <111> orientation translates to the overlying aluminum interconnects, enhancing the Al <111> feature. The improvement of the aluminum texture leads to an appreciable increase in the interconnect median time to failure (MTTF) under electromigration stress conditions.[8] The other favorable qualities of CVD TiN, such as diffusion barrier and nucleation layer characteristics, are retained under these process conditions.

Experimental

The CVD TiN depositions were carried out in a single-wafer cold wall reactor as described elsewhere.[1] The system is a load-locked, single-wafer reactor chamber with a linear cassette to cassette wafer transport. The substrate is radiantly heated from the back side. A thermocouple in contact with the center of the substrate's back side provides closed loop temperature control within ±1% of the set point.

The CVD TiN films were characterized by Auger electron spectroscopy (AES), and scanning electron microscopy (SEM). The crystalline orientation of the CVD TiN films processed under various conditions and that of the overlying Al films were determined using the x-ray diffraction (XRD) technique. The x-ray source was a Cu K_α operated at 45 kV and 40 mA. Both the glancing angle and θ/2θ diffraction methods were used for the crystalline determination. The latter method provides a quick method for determining the crystalline orientation and for checking the film texture. The oxygen, chlorine, and carbon contents were determined from AES. The sheet resistance of the films was measured with a Prometrix Omni map four-point probe (49 points/wafer). The film resistivities were derived from the sheet resistance and the film thickness in the usual manner. The film thicknesses were measured by x-ray fluorescence, calibrated by both cross-sectional transmission electron microscopy (XTEM) and Rutherford backscattering (RBS).

Results and Discussion

Film characteristics.—Traditionally, CVD TiN from $TiCl_3/NH_3$ chemistry has been deposited with $TiCl_4$ partial pressures in the 1.0_4 to 15.0 mTorr range. TiN films deposited under this regime and at elevated temperatures (>550°C) have shown excellent step coverage, near-bulk film density, low chlorine and oxygen concentrations, and a <200> preferred crystal orientation.[1,4] Recent work has shown that CVD TiN films deposited at much lower $TiCl_4$ partial pressure show very different film characteristics.[5] Films deposited at these low $TiCl_4$ partial pressures have shown a TiN <111> preferred orientation, higher oxygen concentrations, and lower chlorine concentrations. However, these films also demonstrate poor step coverage. By the *in situ* layering of film deposited at both high and low $TiCl_4$ partial pressures, a CVD TiN film that is both conformal and <111> preferentially oriented has been developed.